

Cardiac metabolic adaptations in diabetic mice protect the heart from pressure overload-induced failure: a combined *in vivo* MRI, MRS, and PET approach

Desiree Abdurrahim¹, Miranda Nabben¹, Verena Hoerr^{2,3}, Michael T. Kuhlmann⁴, Philipp R. Bovenkamp², Michael Schäfers⁴, Klaas Nicolay¹, Cornelius Faber², Sven Hermann⁴, and Jeanine J. Prompers¹

¹Biomedical NMR, Eindhoven University of Technology, Eindhoven, Netherlands, ²Department of Clinical Radiology, University Hospital Münster, Münster, Germany, ³Institute of Medical Microbiology, Jena University Hospital, Jena, Germany, ⁴European Institute for Molecular Imaging, Münster, Germany

TARGET AUDIENCE: Researchers interested in diabetes and heart failure

PURPOSE: Diabetes patients have a high risk for cardiovascular diseases. Metabolic adaptations in the diabetic heart are proposed as an important contributor to the development of heart failure in diabetes patients. However, data in this field largely originates from *ex vivo* rodent or cross-sectional human studies, which do not allow studying the time course of changes in cardiac metabolism in relation to the decline in cardiac function. We aim to investigate to what extent changes in cardiac metabolic flexibility, lipid accumulation, and energy status predict the longitudinal development of heart failure in non-diabetic and diabetic mice.

METHODS: Animals. Pressure overload heart failure was induced in non-diabetic db/+ and diabetic db/db C57BL/KsJ mice (n=3-10 per group) via transverse aortic constriction (TAC) surgery. Cine MRI, ¹H MRS, ³¹P MRS, and PET were performed at baseline, and at 1, 5, and 12 weeks (wk) after TAC.

MRI/MRS. All measurements were performed using cardiac triggering and respiratory gating, on a 9.4T horizontal bore MR scanner (Bruker Biospin). For MRI and ¹H MRS, a 35-mm quadrature birdcage coil (Bruker Biospin) was used. For ³¹P MRS, a 54-mm linear birdcage coil (Rapid Biomedical) and an actively decoupled surface coil with a diameter of 15 mm were used for transmission and reception, respectively.

Cine MRI. FLASH sequence was used to acquire cine images for 5-6 contiguous short axis and 2 long axis slices (thickness: 1 mm). TR/TE: 7/1.8 ms, α : 15°, matrix: 192x192, FOV: 30x30 mm², frames/cardiac cycle: 15-18, NSA: 6. Left ventricular (LV) lumen was semi-automatically segmented using CAAS MRV 2.0 (Pie Medical) to calculate LV mass and ejection fraction (EF).

¹H MRS. Localized ¹H MR spectra were acquired during diastole in the interventricular septum (1x2x2 mm³ voxel) using the PRESS sequence, with CHESS water suppression, as described previously⁽¹⁾. TR: ~2s, TE: 9.1ms, 0.41 ms 90° Hermite-shaped pulse, 0.9 ms 180° Mao-type pulses, 256 scans. Spectral analysis was performed using AMARES in jMRUI. Cardiac lipid levels were calculated from the lipid-CH₂ signal relative to the unsuppressed water peak.

³¹P MRS. ³¹P MRS was performed using the image selected *in vivo* spectroscopy (ISIS) sequence on a voxel of typically ~6x6x6 mm³ covering the left ventricle, at the end of diastolic phase, as described previously⁽²⁾. TR: ~2s, 1.2 ms sinc-shaped excitation pulse, 6.25 ms adiabatic hyperbolic secant inversion pulses, 96 ISIS cycles (768 scans). Localized shimming was performed on the ¹H signal using an 11x11x11 mm³ PRESS voxel covering the sensitive area of the surface coil. Cardiac energy status was calculated as the PCr/γ-ATP ratio, corrected for T₁ partial saturation.

¹⁸F-FDG PET. To measure myocardial glucose uptake, PET (quadHIDAC; Oxford Positron System) was performed after a 12-13 hour overnight fast. The acquisition was performed for 15 minutes, at one hour after the fluorodeoxyglucose (FDG) injection (~10 MBq). Data was reconstructed into an image volume of 110x60x20 mm³ and a voxel size of 0.4x0.4x0.4 mm³, using a resolution recovery reconstruction algorithm⁽³⁾ leading to an effective resolution of 0.7 mm. Quantification of segmental tracer uptake and volumes of the left ventricle were performed using an automated 3D contour detection algorithm developed in-house.

Statistical analysis. All data are presented as means \pm standard deviation. Statistical analysis was performed using a two-way ANOVA (SPSS Inc), with Bonferroni-corrected post-hoc tests. Statistical significance was set at P<0.05.

RESULTS: Non-diabetic mice: In non-diabetic mice, TAC induced progressive LV hypertrophy (Fig. 1A) and dysfunction (Fig. 1B), which correlated with myocardial FDG uptake (P<0.001). Myocardial FDG uptake was increased at 1 and 5 wk post TAC, but tended to decrease again at 12 wk post TAC (Fig. 1C; Fig. 2). The decrease in FDG uptake at 12 wk post TAC was associated with a trend for lowered cardiac energy status (Fig. 1D). Myocardial lipids were not affected by TAC. **Diabetic mice:** At baseline, diabetic mice had lower myocardial FDG uptake (Fig. 1C), higher myocardial lipid content, and lower myocardial cardiac energy status (Fig. 1D; Fig. 3A-B), but normal cardiac function (Fig. 1B) as compared with non-diabetic mice. Surprisingly, in diabetic mice the effects of TAC on LV mass and function were much less prominent than in non-diabetic mice (Fig. 1A-B). Also in diabetic mice, myocardial FDG uptake increased upon TAC, but it remained lower than in non-diabetic mice (Fig. 1C). Myocardial lipid content and cardiac energy status in diabetic mice (Fig. 1D) were not affected by TAC.

DISCUSSION & CONCLUSION: This study presents the first longitudinal *in vivo* data of cardiac metabolic, energetic, and functional adaptations during heart failure development in non-diabetic and diabetic mice. In non-diabetic mice, the progression to heart failure was correlated with increased myocardial FDG uptake, which preceded the decrease in cardiac energy status. The mild cardiac hypertrophy and dysfunction in diabetic mice, together with lower myocardial glucose uptake upon TAC, suggests that maintaining fatty acid oxidation may be beneficial for cardiac function and energetics in pressure overload-induced heart failure.

REFERENCES: (1) Bakermans AJ. *Magn Reson Med* 2014; doi 10.1002/mrm.25340; (2) Abdurrahim D. *Proc. 21st ISMRM* 2013; 117. (3) Reader A. *IEEE Trans Nucl Sci* 2002;49:693.

ACKNOWLEDGEMENT: D.A. and M.N. contributed equally to this study.

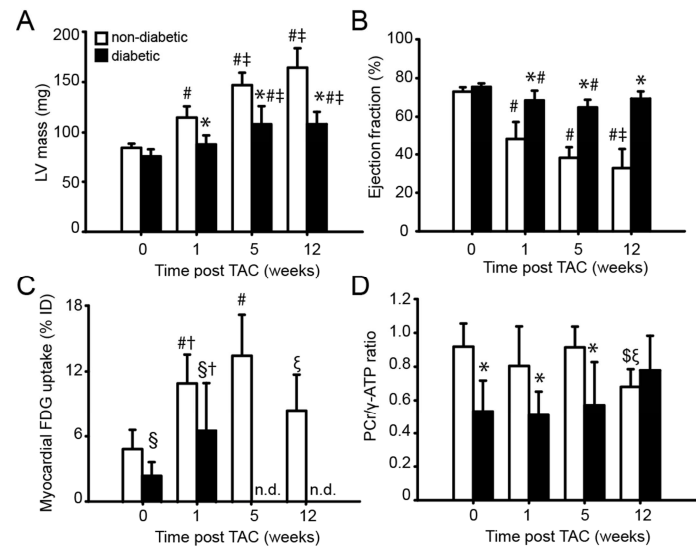


Figure 1. (A) LV mass, (B) ejection fraction, (C) myocardial FDG uptake, and (D) PCr/γ-ATP at baseline, and 1, 5, and 12 wk post TAC. *P<0.05 vs. non-diabetic mice at the same time point, \$P<0.05 vs. non-diabetic mice independent of time. †P<0.05 vs. baseline independent of genotype. For the same genotype: #P<0.05 vs. baseline, ‡P<0.05 vs. 1 week post, ^P<0.05 vs. 5 wk post, \$P<0.10 vs. baseline, ‡P<0.10 vs. 5 wk post TAC. n.d.: data not available.

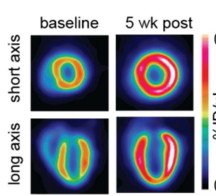


Figure 2. Cardiac FDG-PET images of a non-diabetic mouse at baseline and 5 wk post TAC. ID: injected dose.

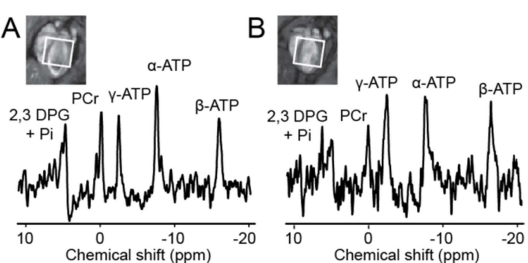


Figure 3. Representative ³¹P MR spectra of a (A) non-diabetic and (B) diabetic mouse at baseline.